Potential Applications of Low Frequency Microwave Measurements of Snow

Richard D. West

Jet Propulsion Laboratory
California Institute of Technology
4800 Oak Grove Drive
Pasadena, California 91109-8099
Phone: 818-354-6025, Fax: 818-393-5184, Email:
Richard.D.West@jpl.nasa.gov

Abstract

Lower frequency microwave radar observations can help to measure the properties of snow cover on land by providing information about the soil-snow boundary condition. In this theoretical study, we examine the sensitivities of microwave radar measurements to soil and snow characteristics, and we compare a simple model with previously published data. Depending on the surface roughness, co-polarized ratios or singe polarization time ratios of radar backscattering may be affected only by the incidence angle and the dielectric contrast at the soil-snow boundary. These measurements can reduce the number of unknowns in any corresponding higher frequency observations which are also affected by the lower boundary condition. The co-polarized ratio is sensitive first of all to the snow density which offers the possibility of measuring this parameter directly if a separate measurement of the soil temperature from a passive microwave system is also available. The thermal insulation provided by snow cover can have a powerful effect on the soil-snow boundary by altering the soil temperature and therefore changing the dielectric contrast. Because the microwave response of snow cover is so sensitive to the conditions of the underlying frozen soil, it is important for future ground truth campaigns that measure snow conditions to also collect data on the temperature, water content, and texture of the soil.

1 Introduction

In this paper, we will examine some potential applications of low frequency microwave radar data to remote sensing of snow cover over land. We focus on the following low frequency bands; L-band (1.28 GHz) and C-band (5.3 GHz). The problem of measuring snow properties with microwave remote sensing instruments is in general very complicated and difficult because of the many physical variables and processes involved. To help clarify the issues involved, we subdivide this large problem according to two categories; dry snow vs. wet snow, and snow cover mapping vs. snow parameter retrieval.

With dry snow, the loss at low microwave frequencies such as L-band is very small so the corresponding penetration depths are very large (eg., 100 m). Clearly seasonal snow covers are far too thin to have a direct scattering or emission effect on these low frequency bands. There are, however, indirect effects introduced because of altered reflection at the soil-snow boundary, and refraction at the snow-air boundary. For C-band, layers of snow with different densities can have an impact if the number of layers grows sufficiently large. (eg., many meters of snow pack with cm-scale density layering [West et al., 1996].)

Wet snow poses a different, more complicated problem. Liquid water is much more effective than ice at scattering and absorbing L- and C-band radiation, so even a small amount of wetness will greatly reduce penetration. For example, with a snow wetness of 1 percent (volume fraction), and a density of 300 kg/m^3, the penetration depths for L-band, and C-band are about 1.6 m, and 0.15 m respectively. Very wet snow can have more than 10 percent liquid water, and the corresponding L-band penetration is less than 0.2 m. Increased dielectric contrast at the snow air boundary makes rough surface scattering at this surface important and introduces more unknowns into the problem [Mätzler and Schanda, 1984].

Mapping snow cover is itself a difficult problem which depends on snow wetness. Wet snow cover has a much lower radar cross-section than many terrain types at lower microwave frequencies and can be mapped on this basis [Mätzler and Schanda, 1984; Baghdadi et al., 1997]. As mentioned earlier, dry snow is transparent at lower microwave frequencies, so much higher frequencies are needed for mapping [Tait et al., 1999]. Optical and infrared sensors are also used for general snow mapping although their coverage is limited to clear sky conditions [Justice et al., 1998; Rosenthal and Dozier, 1996].

To reduce the scope of this paper to a manageable level we will focus on snow parameter retrieval using radar backscatter measurements under dry snow conditions, while keeping in mind the larger context. We further simplify the problem by ignoring the effect of trees and vegetation and concentrate on soil and snow properties. In section 2, we describe the physical model and the parameters and scattering processes which determine the radar backscattering signature. Here we will show that rough surface scattering is the dominant scattering mechanism at L-band for most dry snow conditions, and at C-band for typical dry snow conditions. In section 3, we look at time and polarization ratios

which can be used to reduce the sensitivity of backscattering measurements to the details of the rough surface profile. In particular, we observe that the co-polarization ratio at L-band should be independent of the surface profile if the surface is not too rough. In section 4, we compare results with data collected by Bernier and Fortin [Bernier and Fortin, 1998], and we expand on their discussion of the importance of soil temperatures and the thermal insulation provided by dry snow cover. Finally, in section 5, we summarize the results, and discuss potential applications for low frequency observations of snow.

2 Model Description

To model dry snow cover on soil, we use the physical configuration illustrated in Fig. 1. Snow is represented by a single layer of ice particles in air characterized by a mean density, and a mean snow grain radius. The incidence angle at the snow-air interface is 45° for all of the results in this paper. At L- and C-band, we will be primarily concerned with volume scattering in the snow, and rough surface scattering from the frozen soil. The dielectric constants of the various materials are of fundamental importance in determining the strength of the volume and surface scattering processes, so we discuss them now in more detail. Following the discussion of dielectric constants, we apply simple theoretical models to compute volume and rough surface scattering.

2.1 Snow Dielectric Constant

The real part of the effective relative dielectric constant of dry snow is determined almost completely by the snow density [Mätzler, 1996]. It can be calculated from the formula of Polder and van Satten with some added conditions given by Mätzler [Polder and van Satten, 1946; Mätzler, 1996] that relate the grain structure with the density. The imaginary part is determined by the attenuation rate due to absorption and scattering by the ice particles. We compute the complex dielectric constant using a theoretical calculation called the quasi-crystalline approximation with coherent potential (QCA-CP) which applies to dense random media. [Tsang et al., 1992]. The low frequency solution is used because the Rayleigh scattering limit applies to mm-sized snow grains at L- and C-band. In the low frequency limit, QCA-CP gives the same result as the mixing formula by Polder and van Satten when applied to spheres. This theory has been tested with data from laboratory studies [West et al, 1994; Wen et al, 1990] and with data from snow measurements [Wen et al, 1990; Mandt et al., 1992] which demonstrate that the theory is suitable for typical snow conditions. The principle source of uncertainty is the detailed nature of the snow microstructure. If the snow grains stick together, then the effective size of the scattering units can be larger than the observed grain sizes with commensurately higher scattering levels [Zurk et al., 1996]

The absorption loss comes from the instrinsic loss of the ice particles which has been determined experimentally for the frequencies we are interested in.

The dielectric constants of pure ice at 1.28 and 5.3 GHz respectively are, $3.19 + i0.00073$ and $3.19 + i0.00061$ [Mätzler, 1987]. The imaginary parts which specify the loss due to absorption are slightly temperature dependent, but the variation over typical snow temperatures is too small to cause a noticable change in later results. The scattering loss depends on grain size and leads to a volume scattering contribution to the total radar cross-section (σ_0).

2.2 Soil Dielectric Constant

Frozen soil is assumed to be effectively homogeneous with a dielectric constant determined by the relative proportions of different minerals, ice, and liquid water. If the soil is very dry, then substantial penetration into the soil can occur along with the possibility of volume scattering from rocks and air voids. We assume that the soil is lossy enough that volume scattering effects can be neglected, and we concentrate now on the real part of the soil dielectric constant.

The various mineral phases and ice in frozen soil all have relative dielectric constants in the range $2 - 4$ which are independent of temperature. Liquid water, however, has a much higher dielectric constant of 80 at microwave frequencies. Therefore, even the small amount of liquid water present in soil below freezing can significantly increase its effective dielectric constant. The amount of liquid water in frozen soil is determined by three main factors; the soil temperature, the soil total water content, and the soil texture. In general, texture is less important than temperature and water content, although high clay levels tend to reduce the dielectric constant of soils by binding with some of the free water.

Hallikainen presents experimental data on frozen soil dielectric behavior which we summarize in Fig. 2 [Hallikainen et al., 1984]. These data are for silt-loam soil texture which gives results intermediate between sandy loam and silty clay. After examining this data set, we see that dry soil has a permittivity of about 3 with little dependence on temperature or frequency. Soil with a higher water content, however, shows significant dielectric variation as a function of temperature and frequency. The variation is particularly high at temperatures near the freezing point where the amount of liquid changes rapidly. This behavior is confirmed by soil models [Liou and England, 1996; Ferrand and Sulayman, 1996] by nuclear magnetic resonance experiments [Tice and Oliphant, 1984], and by time domain reflectometer experiments [Stähli and Stadler, 1997; Spaans and Baker, 1995; Hoekstra and Delaney, 1974]. We also call attention to Hallikainens' observation that even at very cold temperatures (eg., -50 C), the high water content soil permittivity is larger than the corresponding low water content soil permittivity. This indicates that some of the water in the soil remains unfrozen, even at very low temperatures. These observations suggest that the temperature and water content of frozen soil will be important variables in determining the dielectric contrast at the soil-snow interface.

The dielectric constant of liquid water follows a debye formula [Mätzler, 1987]. Since the liquid water component has by far the largest frequency dependence, we use a debye-like formula to model the frequency variation of the

	$m_v = 0.048$			$m_v = 0.26$		
T_{soil} (C)	ϵ_∞	ϵ_s	f_0 (GHz)	ϵ_∞	ϵ_s	f_0 (GHz)
-50	2.61	2.78	17.78	3.73	4.22	27.6
-25	2.74	3.18	6.14	3.97	4.63	16.67
-10	2.74	3.22	8.86	4.18	5.13	10.79
-2	2.75	3.37	10.65	4.48	5.70	9.60
0+	2.82	3.58	10.65	5.48	14.18	10.54

Table 1: The Debye parameters fitted to the data presented in Fig. 2

soil dielectric constant.

$$\epsilon'_{soil} = \epsilon_\infty + \frac{\epsilon_s - \epsilon_\infty}{1 + (\frac{f}{f_0})^2}, \tag{1}$$

where ϵ'_{soil} is the real part of the soil dielectric constant, ϵ_∞ is the high frequency limit, ϵ_s is the static limit, and f_0 is the relaxation frequency. These soil parameters can be derived for a given soil water content and temperature using a least squares fit; the results are shown in Table 1. Fig. 2 also shows the resulting fits using these parameters. In the theoretical studies presented in this paper, the dielectric constants of frozen soil are obtained by interpolating the fitted debye constants to the desired temperature and water content, and then evaluating at the desired frequency.

2.3 Volume Scattering in Snow

For the purpose of computing the radar cross-section due to volume scattering $(\sigma_{0(vol)})$ we assume that the soil-snow interface is smooth, and include only specular reflections in the lower boundary condition. Refraction into the snow at the snow-air interface is included, however, reflections at this interface are not included because of the low dieletric contrast. The snow cover is assumed to consist of spherical ice particles in air with a distribution of sizes around the mean radius. The size distribution was obtained from Antarctic data and spans a range of radii from 0.8 to 1.4 times the mean radius [Gow, 1971]. The number density is then scaled to give the desired density which is assumed constant throughout the snow layer. In reality, snow density usually increases slowly with depth, however, the effect of density on volume scattering (see Fig. 4) is much weaker than other effects, and it is approximately linear for densities above 200 kg/m^3 so that replacing the vertical density profile by its mean value will not introduce much error.

Dense medium radiative transport theory (DMRT) with a first order scattering solution is applied to compute $\sigma_{0(vol)}$ [Tsang et al., 1985]. In Figs. 3 and 4 we plot the dependence of $\sigma_{0(vol)}$ on frequency, snow grain size, depth, and snow density. Fig. 3 shows a strong scattering dependence on size and frequency. This occurs because we are in the Rayleigh scattering regime where the scattering cross-section is proportional to f^4a^6 where f is the frequency and

a is the particle radius. From this result, we can see that the detailed nature of the distribution of particle sizes as well as the mean radius will be important in determining the strength of volume scattering. We can also see that at L-band, $\sigma_{0(vol)}$ remains quite low (less than -20 dB with 30 cm of snow) over a wide range of mean grain radius ranging from sub-mm values typical of fresh snow to values near 1 cm which is larger than the sizes present in depth hoar.

Fig. 4 illustrates the dense medium effect where the scattering cross-section rises and then falls slowly with increasing snow density. We can also see that increasing snow depth causes an increase in $\sigma_{0(vol)}$ simply by increasing the amount of scattering material in the round-trip path. The depth dependence of $\sigma_{0(vol)}$ is stronger at higher frequencies because of the strong f^4 frequency dependence. When the depth approaches the scattering path length, $\sigma_{0(vol)}$ will begin to saturate, and the soil-snow interface will no longer be observable [Strozzi et al., 1997]. As long as the depth stays below this limit, there is a possibility of retrieving snow depth from σ_0 measurements. However, as we will see in the next subsection, the total σ_0 is also strongly affected by surface scattering and the characteristics of the frozen soil. For now we note that at C-band $\sigma_{0(vol)}$ remains small (less than -20 dB) for typical snow grains around 1 mm in radius, even with 1 meter of snow. At L-band, the corresponding level is even lower (less that -40 dB). These levels are usually lower than the contribution from rough surface scattering at the soil-snow interface.

2.4 Rough Surface Scattering from the Soil

For the purpose of computing the radar cross-section due to rough surface scattering ($\sigma_{0(surf)}$), we assume that the soil-snow interface is rough with gaussian statistics characterized by the rms height σ, and the correlation length l. Rough surface scattering at the snow-air interface, however, is not included because the low dielectric contrast results in a negligible backscatter contribution compared to the frozen soil surface.

In addition to the surface roughness parameters, the incidence angle and dielectric contrast at the soil-snow interface are important in determining $\sigma_{0(surf)}$. Therefore we include the effect of refraction into the snow at the snow-air interface, and we include an estimate of the effect of snow densification with increasing depth. For the relatively shallow snow covers discussed in this paper, we assume a linear vertical density profile with the surface density set at 200 kg/m^3 which is typical of fresh snow.

To compute $\sigma_{0(surf)}$ we use two simple rough surface scattering theories which apply to two different scattering regimes. For C-band, we use geometric optics with stationary phase (GO) which works when the correlation length is large compared to the wavelength, and the rms height is small compared to the correlation length [Ulaby et al, 1982],

$$kl > 6, \tag{2}$$

$$l^2 > 2.76\sigma\lambda. \tag{3}$$

$$2k\sigma\cos\theta > \sqrt{10}. \tag{4}$$

where k is the wavenumber in the snow, λ is the wavelength in the snow, and θ is the incident angle at the soil surface. The normalized copolarized cross-sections are [Ulaby et al, 1982],

$$\sigma_{0hh} = \sigma_{0vv} = \frac{|R_0|^2}{4\sigma^2/l^2\cos^4\theta}\exp(\frac{-\tan^2\theta}{4\sigma^2/l^2}), \tag{5}$$

where R_0 is the fresnel reflection coefficient at normal incidence.

For L-band, we use the small perturbation method (SPM) which works when the rms height is small compared to the wavelength, and the surface slopes are small [Ulaby et al, 1982],

$$k\sigma < 0.3, \tag{6}$$

$$\frac{\sqrt{2}\sigma}{l} < 0.3. \tag{7}$$

The normalized copolarized cross-sections are [Ulaby et al, 1982],

$$\sigma_{0pp} = 4k^4\sigma^2l^2\cos^4\theta|\alpha_{pp}|^2\exp(-k^2l^2\sin^2\theta), \tag{8}$$

where $\epsilon_r = \epsilon_{soil}/\epsilon_{snow}$ is the relative dielectric contrast at the soil-snow interface, $p = v, h$ to specify the polarization, and,

$$\alpha_{hh} = R_h, \tag{9}$$

$$\alpha_{vv} = (\epsilon_r - 1)\frac{\sin^2\theta - \epsilon_r(1+\sin^2\theta)}{(\epsilon_r\cos\theta + \sqrt{\epsilon_r - \sin^2\theta})^2}, \tag{10}$$

where R_h is the fresnel reflection coefficient for horizontal polarization.

The SPM and GO models have been tested against measurements of bare soil surfaces and found to be in reasonable agreement for incidence angles less than 50 degrees, although, there is some indication that the copolarization ratio $\sigma_{0vv}/\sigma_{0hh}$ predicted by SPM may be too large [Yisok et al., 1992; Fung et al., 1992]. For some natural surfaces, an exponential correlation function may be more appropriate than the gaussian correlation function that we assume [Yisok et al., 1992], however, this does not affect the conclusions that we draw later on. Fig. 5 shows sample theoretical backscattering results using some representative parameters. The snow density must be accounted for because the larger propagation constant compared to air shifts the wavelength to a shorter value which makes the surface appear rougher than it would without the snow. The snow also alters the incidence angle by refraction which again changes the surface backscattering when compared to snow free areas. In general, $\sigma_{0(surf)}$ is a function of both σ and l, as well as the dielectric contrast and incidence angle at the boundary. Note that $\sigma_{0(surf)}$ is above -20 dB except for very smooth surfaces, and in the geometric optics regime, the surface backscatter can be higher than -10 dB (at 45 deg. incidence). These values are much higher than the volume scattering contribution expected at L-band for modest snow covers

(see Fig. 3). Snow usually has a mean grain radius of less than 1 mm, which implies a $\sigma_{0(vol)}$ less than -40 dB with up to 1 meter of snow. Even if depth hoar is present with grains approaching 5 mm in radius, $\sigma_{0(vol)}$ remains below -30 dB at L-band with 30 cm of snow cover. Only in the extreme case of 1 meter of depth hoar with 1 cm diameter ice grains does $\sigma_{0(vol)}$ increase to -27 dB which is comparable to $\sigma_{0(surf)}$ for very smooth surfaces. Thus, for most conditions with snow cover depths less than 1 meter, we expect that L-band σ_0 will be dominated by surface scattering at the soil-snow interface, with a negligible contribution coming from volume scattering in the dry snow cover.

C-band surface scattering is usually in the geometric optics regime where $\sigma_{0(surf)}$ is higher than at L-band which usually lies in or close to the SPM regime. However, $\sigma_{0(vol)}$ is also higher at C-band because of the f^4 dependence of Rayleigh scattering. Thick snow layers or depth hoar can raise $\sigma_{0(vol)}$ to levels comparable to $\sigma_{0(surf)}$ which complicates the C-band backscattering signature when these conditions occur.

At still higher frequencies such as Ku-band $\sigma_{0(vol)}$ is comparable to $\sigma_{0(surf)}$ for typical snow conditions (compare Fig. 3 with the GO results in Fig. 5). This complicates the dependence of higher frequency radar measurements on snow parameters. However, higher frequencies have the advantage of being more directly sensitive to the snow depth if the complications can be sorted out.

3 Backscattering Ratios and Sensitivities

As Fig. 5 shows, $\sigma_{0(surf)}$ is a function of both σ and l for both SPM and GO. These two unknowns can vary independent of snow conditions, thus introducing a source of error when we attempt to retrieve snow parameters. One way to reduce the dependence of the measurements on the soil roughness parameters is to form ratios of σ_0. The most obvious choice is to form the copolarized ratio which we define to be $\sigma_{0vv}/\sigma_{0hh}$. With SPM the copolarized ratio is,

$$\frac{\sigma_{0vv}}{\sigma_{0hh}} = \frac{|\alpha_{vv}|^2}{|\alpha_{hh}|^2}. \tag{11}$$

We see that the SPM copolarized ratio is independent of σ and l, and depends only on the incidence angle and the dielectric contrast at the soil-snow interface. Thus, multi-polarization measurements at low frequencies like L-band which fall in or close to the SPM regime offer the special advantage of theoretical insensitivity to the rough surface parameters.

In the GO regime, the copolarized ratio is always 1.0 and does not offer any useful information. An alternative choice is to define a time ratio between the σ_0 measured with snow to the σ_0 measured at the same location without snow, and assume that the surface roughness remains unchanged. For GO we have,

$$\frac{\sigma_{0(snow)}}{\sigma_{0(bare)}} = \frac{\cos^4\theta_{bare}}{\cos^4\theta_{snow}} \frac{|R_{0(snow)}|^2}{|R_{0(bare)}|^2} \exp\left(\frac{-(\tan^2\theta_{snow} - \tan^2\theta_{bare})}{4\sigma^2/l^2}\right), \tag{12}$$

and for SPM we have,

$$\frac{\sigma_{0pp(snow)}}{\sigma_{0pp(bare)}} = \frac{\cos^4\theta_{snow}}{\cos^4\theta_{bare}} \frac{|\alpha_{pp(snow)}|^2}{|\alpha_{pp(bare)}|^2} \exp(-k^2l^2(\sin^2\theta_{snow} - \sin^2\theta_{bare})). \quad (13)$$

These time ratios are restricted to areas of seasonal snow cover, and are limited by the assumption of invariant surface conditions. On the other hand, they have the advantage of working for both GO and SPM, and they can be used with single polarization measurements. The time ratios reduce the dependence on σ and l by dividing out their direct contribution for both SPM and GO. Unfortunately, the change of incidence angle due to refraction into the snow maintains an exponential dependence on σ and l in both cases.

In the GO regime, if the mean squared surface slope s^2 is sufficiently large,

$$s^2 = 2\frac{\sigma^2}{l^2} >> \frac{\tan^2\theta_{snow} - \tan^2\theta_{bare}}{2}, \quad (14)$$

then the exponential term in the time ratio is close to unity and we have,

$$\frac{\sigma_{0(snow)}}{\sigma_{0(bare)}} \approx \frac{|R_{0(snow)}|^2}{|R_{0(bare)}|^2} \frac{\cos^4\theta_{bare}}{\cos^4\theta_{snow}}. \quad (15)$$

which depends only on the dielectric contrast and the shift in incidence angle. We see evidence of this in Fig. 5 which shows the GO σ_0 saturating with increasing σ. Thus, for a subset of the GO regime, the time ratio is insensitive to the rough surface parameters. For an incidence angle of 45 deg., and snow density of 300 kg/m^3, this subset is restricted to surfaces where $kl, k\sigma > 18$ and $\sigma > l$. At a low frequency like C-band these conditions imply surfaces that have relatively large undulations where $l, \sigma > 20$ cm.

Figs. 6, 7, and 8 show both the time ratio for GO and SPM, and the copolarized ratio for SPM as a function of the snow and soil parameters that determine the dielectric contrast and the incidence angle shift. In Fig. 6 we see that increasing the soil temperature brings the time ratios closer to unity because the dielectric contrast between soil and snow is increased, bringing it closer to the reference contrast of 1:18. Most of the increase occurs at temperatures close to the freezing point because the liquid water content in the soil changes most rapidly here. We also see that the SPM copolarized ratio is much less sensitive to changes of the soil dielectric constant than the time ratios are (1.2 dB vs. 5.3 dB). This difference occurs because the dielectric change affects both the numerator and denominator of the copolarized ratio and is partially cancelled, while only the numerator of the time ratio is affected so there is no cancellation. Finally, we see that typical variations in σ can cause comparable or larger changes in the GO time ratios compared to the changes caused by soil temperature variation.

Fig. 7 shows the corresponding results as a function of soil total water content. The same basic observations can be made for this figure as for Fig. 6 because the soil total water content also affects the soil dielectric constant.

The variation is smooth over the plotted range because the soil dielectric model interpolates between the two sampled water content values (0.048 and 0.26), however, future experiments may uncover more complicated structure.

Fig. 8 shows the variation of the σ_0 ratios as a function of snow density. The SPM copolarized ratio now shows a stronger variation of 2.4 dB over the typical range of 100 to 500 kg/m^3. Snow density affects the copolarized ratio more than soil dielectric changes because it affects the incidence angle as well as the surface response. The time ratios also show strong variation with snow density, but we still have the equally strong dependence on rough surface parameters. The copolarized ratio is clearly more useful than the time ratios for tracking the snow density because it is contaminated by fewer additional variables. In some cases, however, we have to use time ratios because SPM does not apply, or multi-polarization data is not available.

4 Comparison with Data

In this section, we examine aircraft C-band SAR data and associated ground truth collected and analyzed by [Bernier and Fortin, 1998]. The ground truth data included the surface roughness parameters; $\sigma = 2.48cm$ and $l = 6.52cm$. These values fall within the GO regime at C-band, and knowing them separate from the σ_0 measurements allows the use of time ratios without having to account for unknown surface roughness parameters. Following the same approach used by Bernier and Fortin, we compute total σ_0 as a combination of surface scattering from the soil-snow interface and volume scattering in the snow. We use dense medium theory to compute the volume scattering instead of independent scattering theory as used by Bernier and Fortin. Dense medium theory predicts a much lower level of volume scattering than independent scattering [Wen et al, 1990], however, in this case the total σ_0 is dominated by rough surface scattering whether dense medium theory or independent scattering theory is used to compute the volume scattering contribution.

The data presented by Bernier and Fortin includes information about the mean snow density and depth which we incorporate into the physical model described in section 2. Fig. 9 shows a comparison of model results with the data collected by Bernier and Fortin. The data are plotted against snow thermal resistance to match the appearance of Fig. 11 in [Bernier and Fortin, 1998]. The snow depth and density are obtained from the thermal resistance and the snow water equivalent (from Fig. 7 in [Bernier and Fortin, 1998]). The underlying soil is assumed to have a fixed volumetric water content of 0.26. This assumption corresponds to fairly wet soil and allows the model to reproduce the dynamic range of the data with a reasonable range of soil temperatures.

The soil temperature is fit to the observed time ratios in two steps. First, a dielectric contrast is fit in the least squares sense to the observed time ratios. Since the snow density is known, the dielectric contrast gives the required soil dielectric constant. Once the soil dielectric constant and total water content are fixed, the corresponding temperature is derived from the debye formulas fit to

Hallikainens' data for silt-loam (see Fig. 2). Fig. 10 shows the soil dielectric constants that generate the model results shown in Fig. 9, and Fig. 11 shows the soil temperatures that correspond to the fitted soil dielectric constants and the model results shown in Fig. 9.

We have assumed a fixed soil water content and texture even though these parameters are probably varying somewhat between data points, so there is some model uncertainty in the fitted soil temperatures. Furthermore, soil temperatures in the model were constrained to lie between 0 C and -10 C to avoid unreasonable fits. As a result, some of the very low and very high observed ratios were not fit very well. These points could be fit by allowing the soil water content and the soil texture to vary, but no specific information on these parameters is available, so we leave the fit as is.

Bernier and Fortin also collected some soil temperature data (see Fig. 8 in [Bernier and Fortin, 1998]) which varies with the σ_0 time ratio. They also observed a logarithmic relation between snow thermal resistance and the observed time ratios. We use the same logarithmic relation, time ratio = $3.9 \log(\text{thermal resistance}) - 4.3$, to estimate the corresponding thermal resistance values for the four measured temperature levels. These points are shown as "*" symbols in Fig. 11. The model temperatures are consistent with the available measurements, and most of the points are a few degrees C below 0 which is typical for frozen soil. These results indicate that the physical model and the scattering model are consistent with the data, and that they capture the important parameters and scattering processes.

5 Conclusions

Scattering and emission at L- and C-band are dominated by rough surface scattering from the soil-snow interface for typical dry snow conditions, with volume scattering becoming more important at C-band when large snow grains (depth hoar) or thicker (> 1 meter) snow covers are present. At higher frequencies, volume scattering in the snow pack becomes an important contributor to the total σ_0 which increases the number of geophysical parameters needed to model the backscatter. Although low frequency microwave observations are not directly sensitive to snow depth, they can make an important contribution by measuring the dielectric contrast at the soil-snow interface. This reduces the number of unknowns in any corresponding higher frequency observations which are also affected by the lower boundary condition. Also, the copolarized ratio at L-band is sensitive first of all to the snow density which offers the possibility of measuring this parameter directly (see for example the work of [Shi and Dozier, 1996]). The affect of soil temperature, however, appears to be a significant source of error when attempting to retrieve snow density from L-band backscattering. Therefore, an independent estimation of the soil temperature using coincident passive microwave observations (also at low frequency) will probably be needed. The accuracy requirements for such active and passive measurements will be quite stiff ($\delta\sigma_0 << 1\ dB$, and $\delta T << 1\ K$), otherwise the snow density signal

will be washed out by random noise.

As pointed out in [Bernier and Fortin, 1998], the thermal insulation provided by snow cover can have a powerful effect on the soil-snow interface by altering the soil temperature and therefore changing the dielectric contrast. The size of this effect depends on many factors including the temperature difference between the air and the soil at depth, the density of the snow, and the thermal properties of the soil. All of these factors will vary with time and location. In cases where the insulation effect is strong, it may appear that snow depth is directly affecting low frequency microwave backscattering even though in reality it is the dielectric constant of the soil which is changing. Because the microwave response of snow cover is so sensitive to the conditions of the underlying frozen soil, it is important for future ground truth campaigns that measure snow conditions to also collect data on the temperature, water content, and texture of the soil. This will help to separate the volume scattering effects in the snow from the effects of surface scattering at the soil-snow interface.

6 Acknowledgments

This work was performed under contract with the National Aeronautics and Space Administration at the Jet Propulsion Laboratory, California Institute of Technology. The author would particularly like to thank Dr. Simon Yueh for his encouragement of this work, and for the help of many technical discussions.

References

[1] N. Baghdadi, Y. Gauthier, and M. Bernier, "Capability of multitemporal ERS-1 SAR data for wet-snow mapping," Remote Sensing of Environment, vol 60, no. 2, pp. 174-186, 1997.

[2] M. Bernier and J. Fortin, "The potential of times series of C-band SAR data to monitor dry and shallow snow cover," IEEE Trans. on GeoScience and Remote Sensing, vol. 36, no. 1, pp. 226-243, Jan 1998.

[3] L. A. Ferrand and J. A. Sulayman, "A computational investigation of some effects of temperature on soil moisture," Water Resources Research, vol. 32, no. 12, pp. 3429-3436, Dec 1996.

[4] A. K. Fung, Z. Li, and K. S. Chen, "Backscattering from a randomly rough dielectric surface," IEEE Trans. on GeoScience and Remote Sensing, vol. 30, no. 2, pp. 356-369, Mar 1992.

[5] A. J. Gow, "Depth-Time-Temperature relationships of ice crystal growth in polar glaciers," Corps of Engineers, U.S. Army, Cold Regions Research and Engineering Laboratory, Hanover, NH, 1971.

[6] M. Hallikainen, F. T. Ulaby, M. C. Dobson, and M. El-Rayes, "Dielectric measurements of soils in the 3- to 37-GHz band between -50 C and 23 C," Proceedings of IGARSS 1984 Symposium; Strasbourg, pp. 163-168, Aug 1984.

[7] P. Hoekstra and A. Delaney, "Dielectric properties of soils at UHF and microwave frequencies," J. Geophysical Research, vol. 79, no. 11, pp. 1699-1708, Apr 1974.

[8] C. O. Justice, E. Vermont, J. R. G. Townshend, R. Defries, D. P. Roy, D. K. Hall, V. V. Salomonson, J. L. Privette G. Riggs, A. Strahler, W. Lucht, R. B. Myneni, Y. Knyazikhin, S. W. Running, R. R. Nemani, Z. Wan, A. R. Huete, W. Leeuwen, R. E. Wolfe, L. Giglio, J. Muller, P. Lewis, and M. J. Barnsley, "The moderate resolution imaging spectroradiometer (MODIS): land remote sensing for global change research," IEEE Trans. on GeoScience and Remote Sensing, vol. 36, no. 4, pp. 1228-1249, Jul 1998.

[9] Y. Liou and A. W. England, "Annual temperature and radiobrightness signatures for bare soils," IEEE Trans. on GeoScience and Remote Sensing, vol. 34, no. 4, pp. 981-990, Jul 1996.

[10] C. Mätzler and E. Schanda, "Snow mapping with active microwave sensors," Int. J. Remote Sensing, vol 5, no. 2, pp. 409-422, 1984.

[11] C. Mätzler, "Applications of the interaction of microwaves with the natural snow cover," Remote Sensing Reviews, 2, pp. 259-387, 1987.

[12] C. Mätzler, "Microwave permittivity of dry snow," IEEE Trans. on Geo-Science and Remote Sensing, vol. 34, no. 2, pp. 573-581, Mar 1996.

[13] C. E. Mandt, Y. Kuga, L. Tsang, and A. Ishimaru, "Microwave propagation and scattering in a dense distribution of non-tenuous spheres: experiment and theory," Waves in Random Media, vol. 2, pp. 225-234, 1992.

[14] D. Polder, and J. H. van Satten, "The effective permeability of mixtures of solids," Physica, vol. 12, pp. 257-271, 1946.

[15] W. Rosenthal and J. Dozier, "Automated mapping of montane snow cover at subpixel resolution from the Landsat Thematic Mapper," Water Resources Research, vol. 32, no. 1, pp. 115-130, Jan 1996.

[16] J. Shi and J. Dozier, "Estimation of snow water equivalence using SIR-C/X-SAR," Proceeding of IGARSS 1996, pp. 2002-2004, 1996.

[17] E. J. A. Spaans, and J. M. Baker, "Examining the use of time domain reflectometry for measuring liquid water content in frozen soil," Water Resources Research, vol. 31, no. 12, pp. 2917-2925, Dec 1995.

[18] M. Stähli and D. Stadler, "Measurement of water and solute dynamics in freezing soil columns with time domain reflectometry," J. of Hydrology, vol. 195, pp.352-369, 1997.

[19] T. Strozzi, A. Wiesmann, and C. Mätzler, "Active microwave signatures of snow covers at 5.3 and 35 GHz," Radio Science, vol. 32, no. 2, pp. 479-495, Mar-Apr 1997.

[20] A. Tait, D. Hall, J. Foster, A. Chang, and A. Klein, "Detection of snow cover using millimeter-wave imaging radiometer (MIR) data," Remote Sensing of Environment, vol 68, no. 1, pp. 53-60, 1999.

[21] A. R. Tice and J. L. Oliphant, "The effects of magnetic particles on the unfrozen water content of frozen soils determined by nuclear magnetic resonance," Soil Science, vol. 138, no. 1, pp. 63-73, Jul 1984.

[22] L. Tsang, J. A. Kong, and R. T. Shin, *Theory of Microwave Remote Sensing*, New York: Wiley-Interscience, 1985.

[23] L. Tsang, C. Mandt, and K. Ding, "Monte Carlo simulations of extinction rate of dense media with randomly distributed dielectric spheres based on solution of Maxwell's equations," Optics Letters, pp. 314-316, 1992.

[24] F. T. Ulaby, R. K. Moore, and A. K. Fung, *Microwave Remote Sensing, Vol II*, Addison-Wesley Publishing Company, Reading, Massachusetts, 1982.

[25] B. Wen, L. Tsang, D. P. Winebrenner, and A. Ishimaru, "Dense medium radiative transfer theory: comparison with experiment and application to microwave remote sensing and polarimetry. IEEE Trans. on GeoScience and Remote Sensing, vol. 28, no. 1, pp. 46-59, Jan 1990.

[26] R. D. West, D. Gibbs, L. Tsang, and A. K. Fung, "Comparison of optical scattering experiments and the quasi-crystalline approximation for dense media," Journal of the Optical Society of America A, vol. 11, no. 6, pp. 1854-1858, Jun 1994.

[27] R. D. West, D. P. Winebrenner, and L. Tsang, "Microwave emission from density-stratified Antarctic firn at 6 cm wavelength," J. of Glaciology, vol. 42, pp. 63-76, 1996.

[28] O. Yisok, K. Sarabandi, and F. Ulaby, "An empirical model and an inversion technique for radar scattering from bare soil surfaces," IEEE Trans. on GeoScience and Remote Sensing, vol. 30, no. 2, pp. 370-381, Mar 1992.

[29] L. M. Zurk, L. Tsang, and D. P. Winebrenner, "Scattering properties of dense media from Monte Carlo simulations with application to active remote sensing of snow," Radio Science, vol. 31, no. 4, pp. 803-819, Jul-Aug 1996.

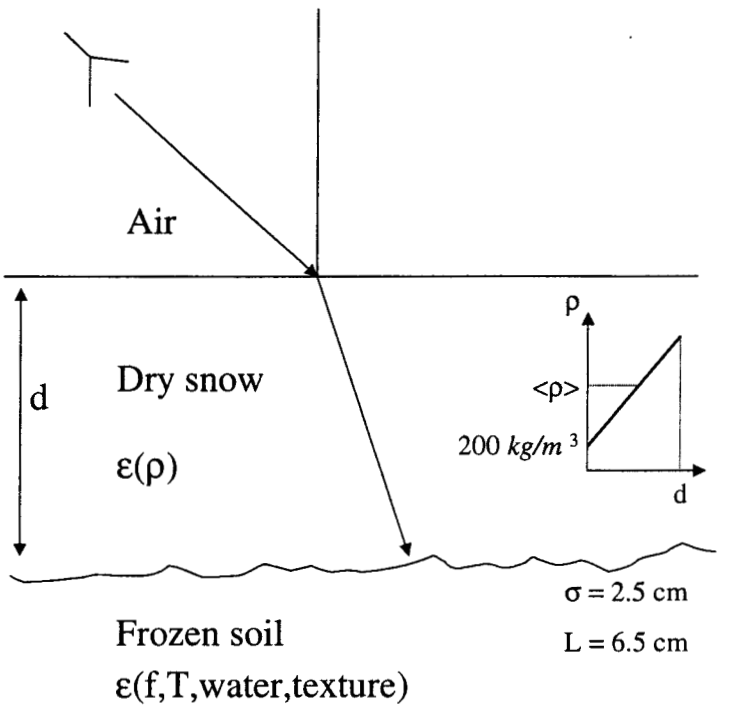

Figure 1: Physical Configuration used to model dry snow over frozen soil. Air/snow boundary is assumed to be flat while the soil-snow boundary is assumed to be a gaussian rough surface with rms height = 2.5 cm and a correlation length of 6.5 cm. The snow density profile is linear starting at 200 kg/m^3 and increasing to give the specified mean density.

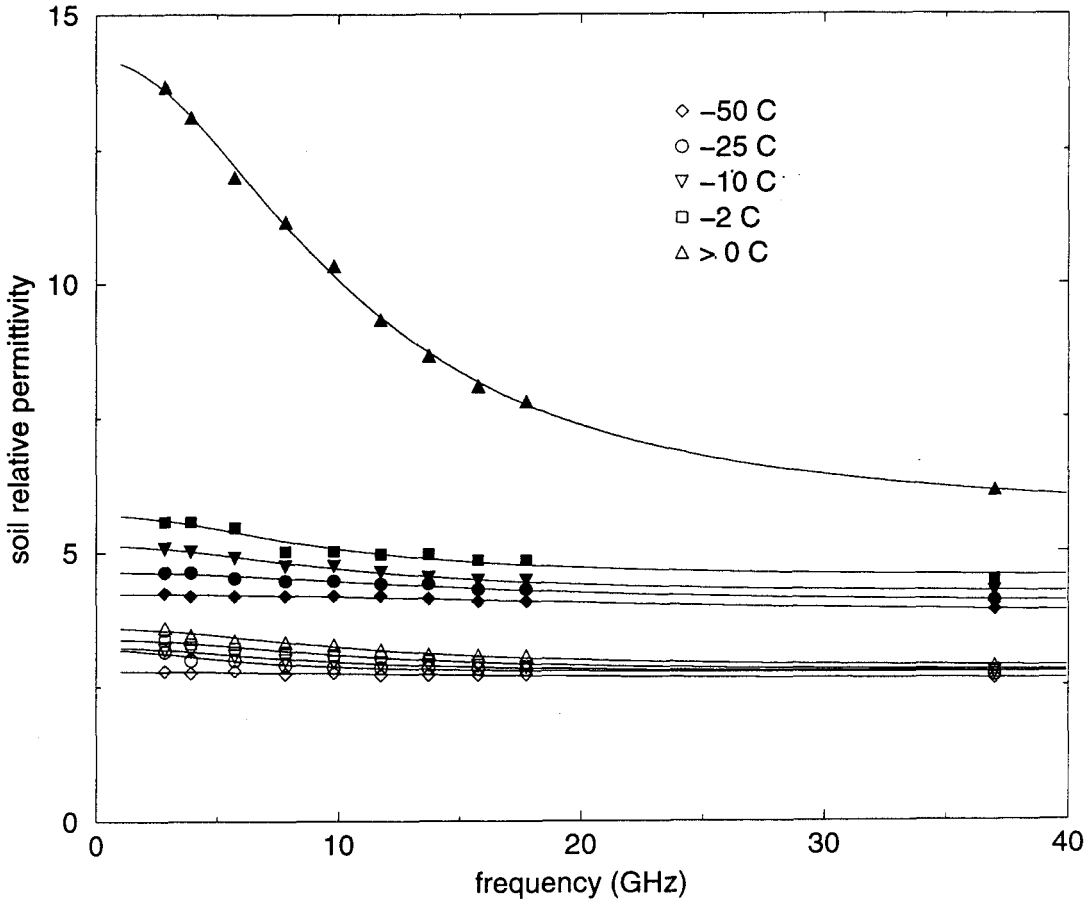

Figure 2: Permittivity of frozen soil as a function of frequency, temperature, and volumetric water content. These data were measured by Hallikainen and presented in Figs. 3 and 5 of [Hallikainen et al., 1984]. We show only the results for silt-loam texture. The filled symbols correspond to a soil volumetric water content of 0.26, while the open symbols correspond to a soil volumetric water of 0.048. The lines show Debye fits using the parameters in Table 1.

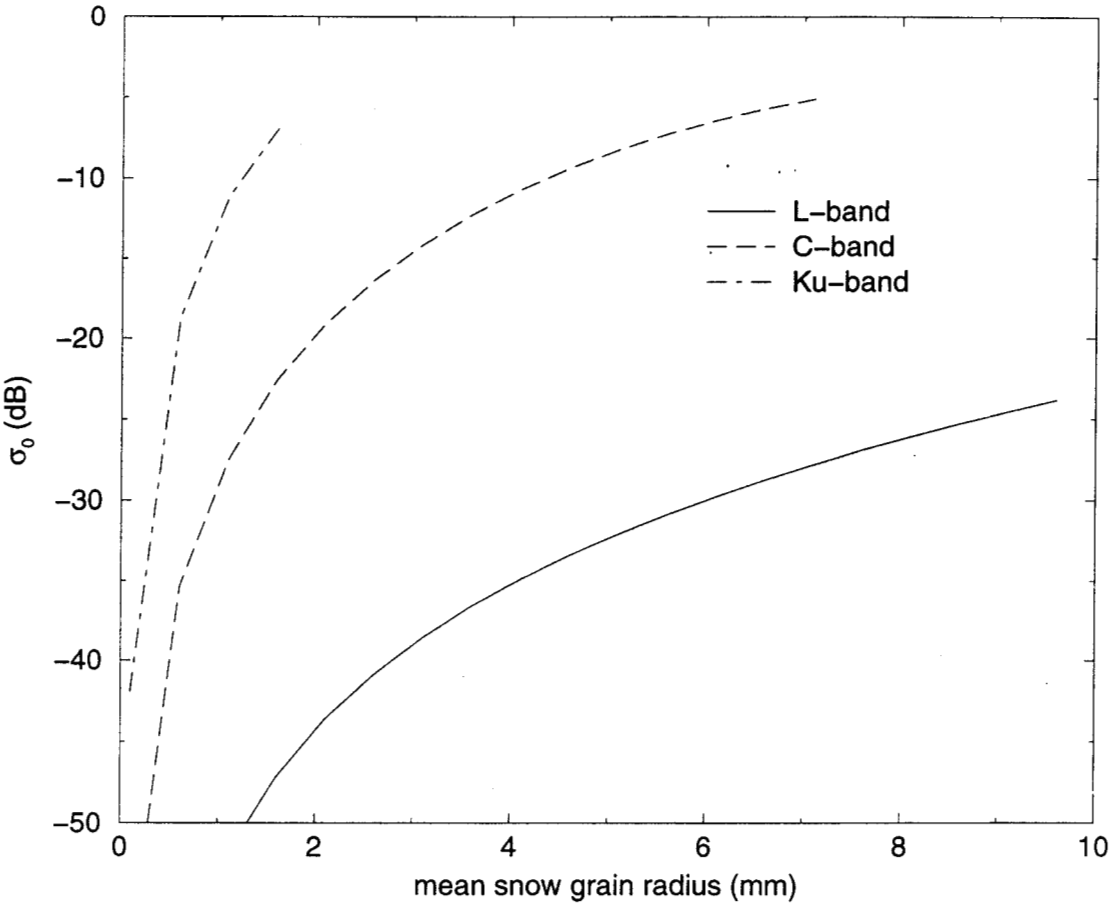

Figure 3: Volume scattering $\sigma_{0(vol)}$ as a function of mean snow grain radius for three different frequencies (Ku-band – 14 GHz, C-band – 5.3 GHz, L-band – 1.28 GHz). Other parameters: snow density = 300 kg/m^3, snow temperature = -10 C, snow depth = 30 cm, soil temperature = -3 C, soil volumetric water content = 0.25, incidence angle = 45°. First order scattering theory is used.

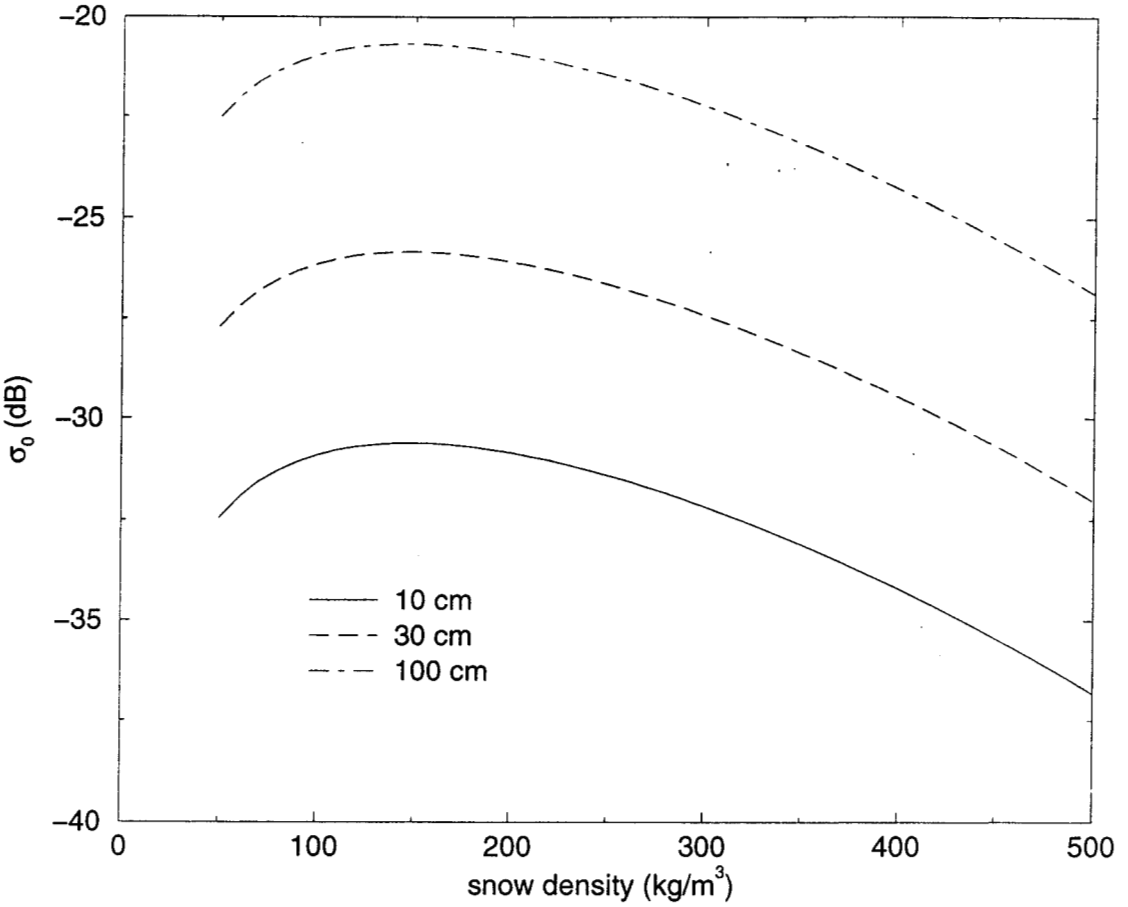

Figure 4: Volume scattering $\sigma_{0(vol)}$ as a function of mean snow density for three different snow depths. Other parameters: frequency = 5.3 GHz, snow grain mean radius = 1.1 mm, snow temperature = -10 C, soil temperature = -3 C, soil volumetric water content = 0.25, incidence angle = 45°.
First order scattering theory is used.

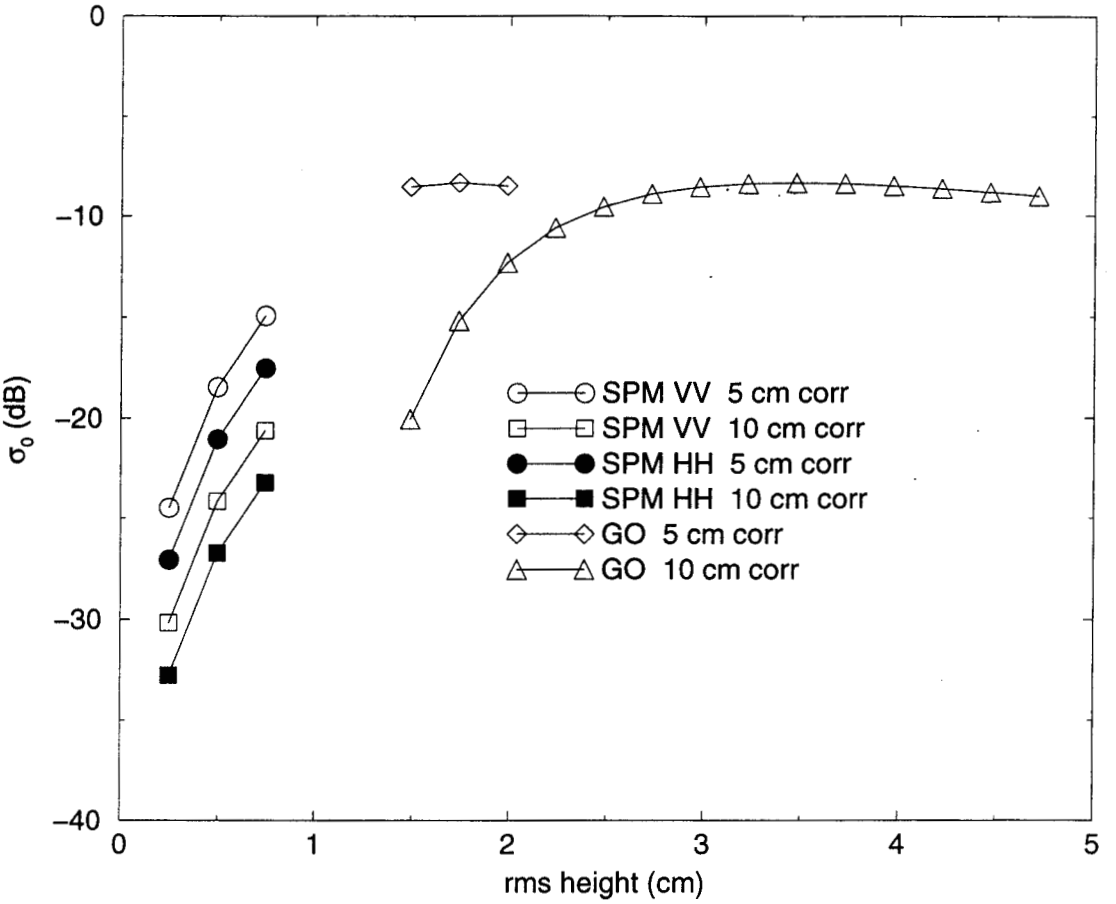

Figure 5: Rough surface scattering $\sigma_{0(surf)}$ as a function of rms surface height σ for small perturbation theory (VV and HH), and geometric optics using two different correlation lengths. Other parameters: frequency = 1.28 GHz for SPM results, frequency = 5.3 GHz for GO results, snow grain density = 300 kg/m^3, snow temperature = -10 C, snow wetness = 0, resulting snow permittivity = 1.55, incidence angle = 45°. soil temperature = -3 C, volumetric soil wetness = 0.25, resulting soil permittivity = 5.26.

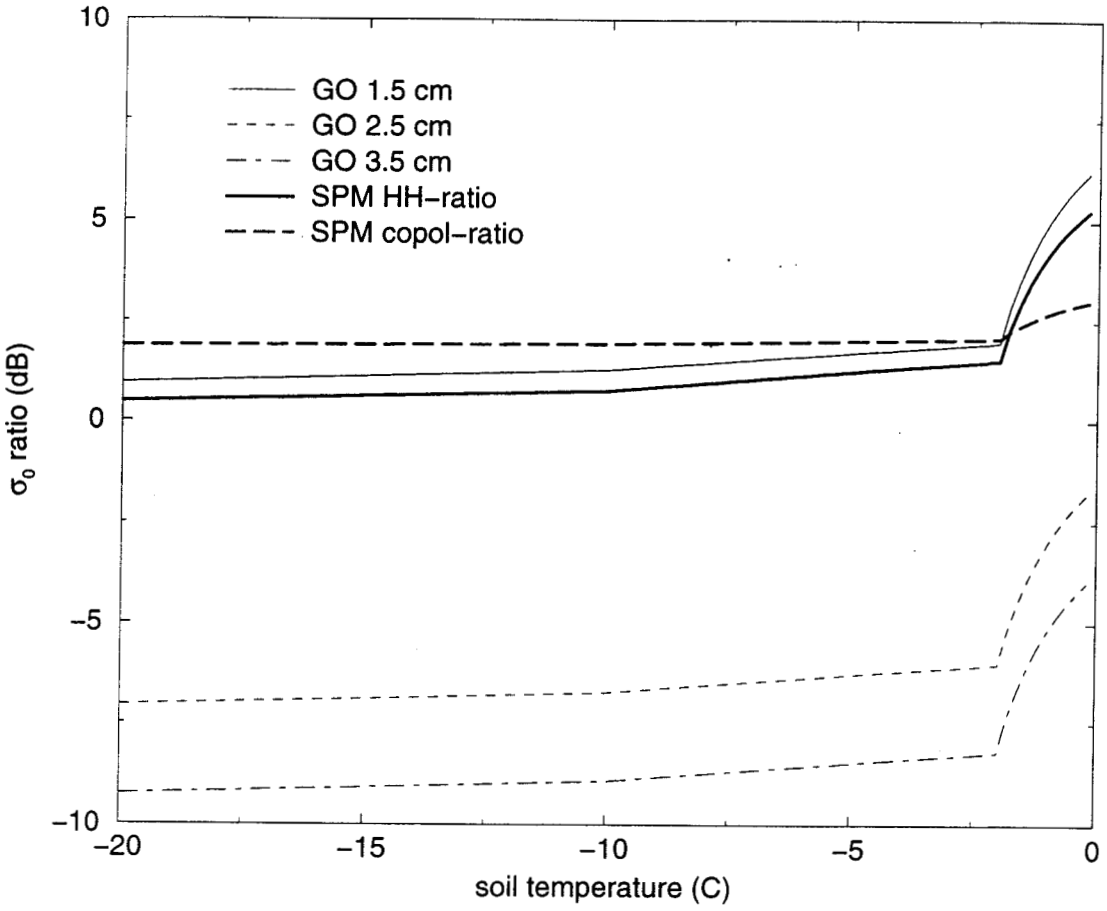

Figure 6: Time and polarization σ_0 ratios as a function of soil temperature for three different rms surface heights. The correlation length is 6.52 cm, which makes the geometric optics under stationary phase (GO) approximation valid at C-band (5.3 GHz, thin lines) for the three rms heights. The small perturbation method (SPM) ratios are unaffected by the surface roughness parameters within the valid domain of the SPM. SPM results are run at L-band (1.28 GHz, thick lines). Other parameters: snow density = 400 kg/m^3, snow temperature = -10 C, snow depth = 30 cm, snow grain mean radius = 1 mm, soil volumetric wetness = 0.25 cm^3/cm^3, incidence angle = 45°. Reference soil permittivity = 18 for the time ratios which are formed for $\sigma_0(hh)$. Copol ratios are defined to be $\sigma_0(vv)/\sigma_0(hh)$.

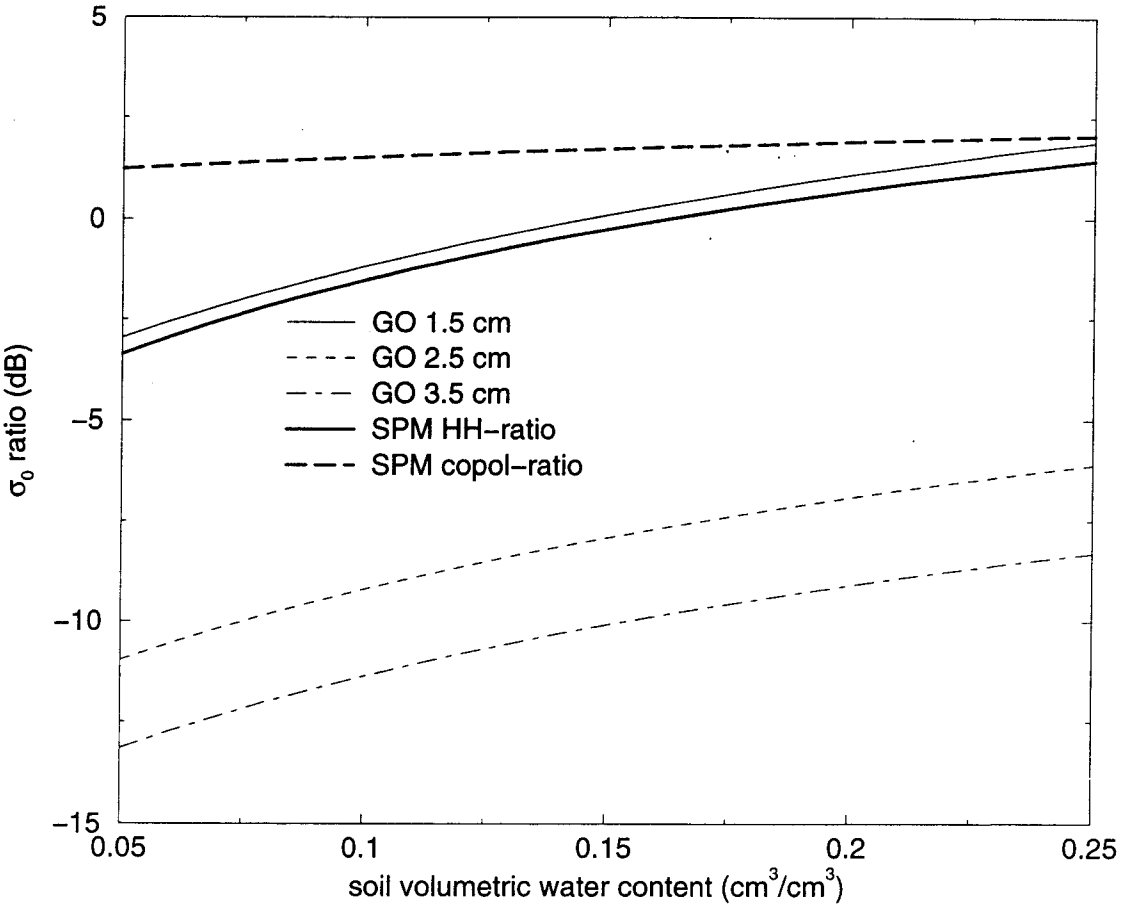

Figure 7: Time and polarization σ_0 ratios as a function of soil volumetric wetness for three different rms surface heights. Other parameters: snow density = 400 kg/m^3, snow temperature = -10 C, snow depth = 30 cm, snow grain mean radius = 1 mm, soil temperature = -3 C, incidence angle = 45°.

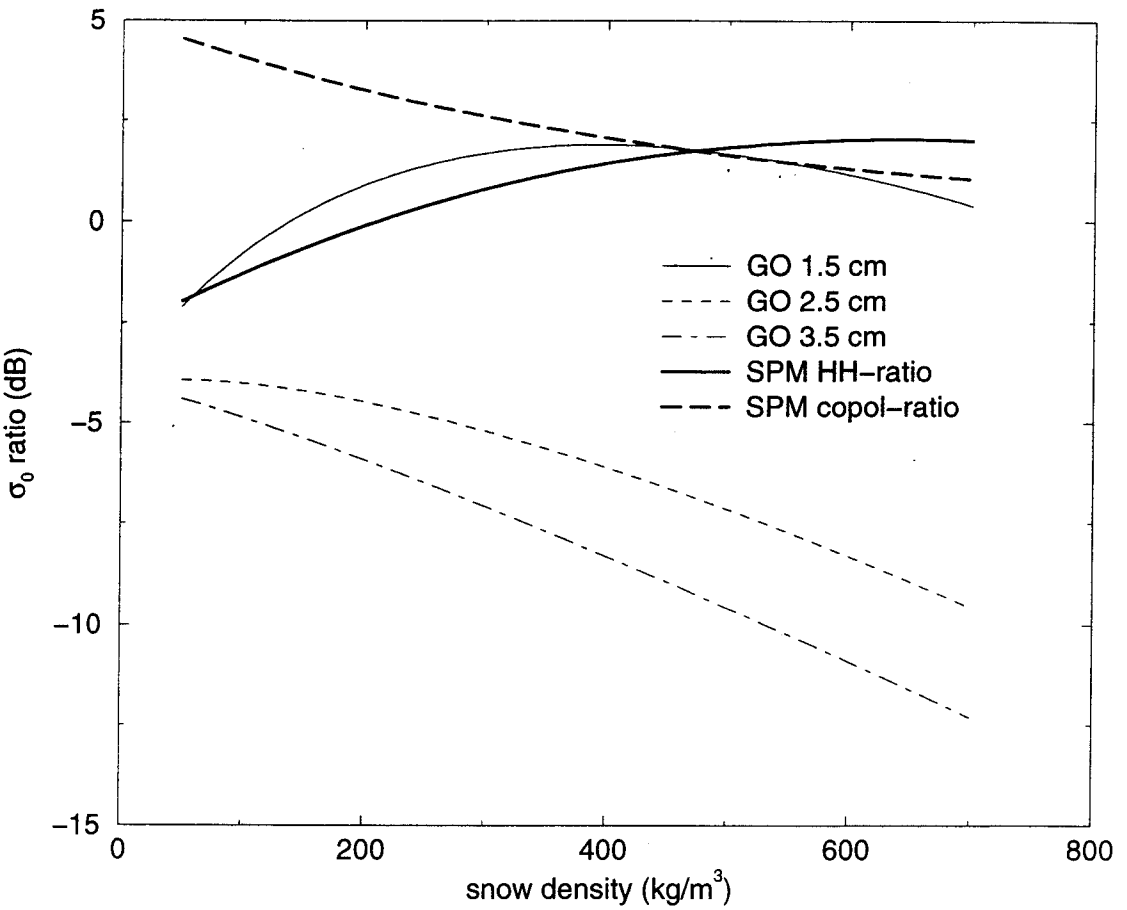

Figure 8: Time and polarization σ_0 ratios as a function of snow density for three different rms surface heights. Other parameters: snow density = 400 kg/m^3, snow temperature = -10 C, snow depth = 30 cm, snow grain mean radius = 1 mm, soil volumetric wetness = 0.25 cm^3/cm^3, soil temperature = -3 C, incidence angle = 45°.

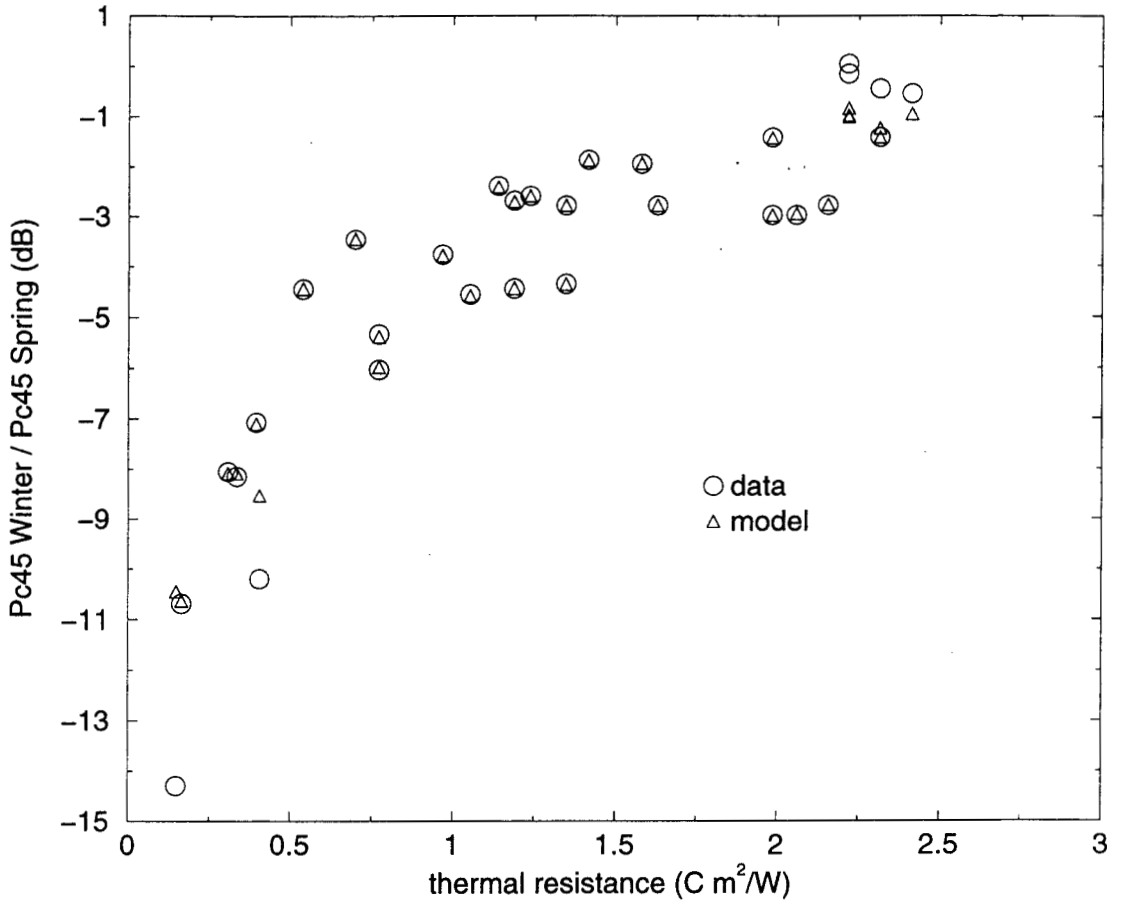

Figure 9: Comparison of data [Bernier and Fortin, 1998] with model results generated using the measured snow depth and average density, and fitting the soil temperature for an assumed constant soil water content. The snow density profile is assumed to start at 200 kg/m^3 at the surface and increase linearly with depth to give the observed mean density. Incidence angle = 45°.

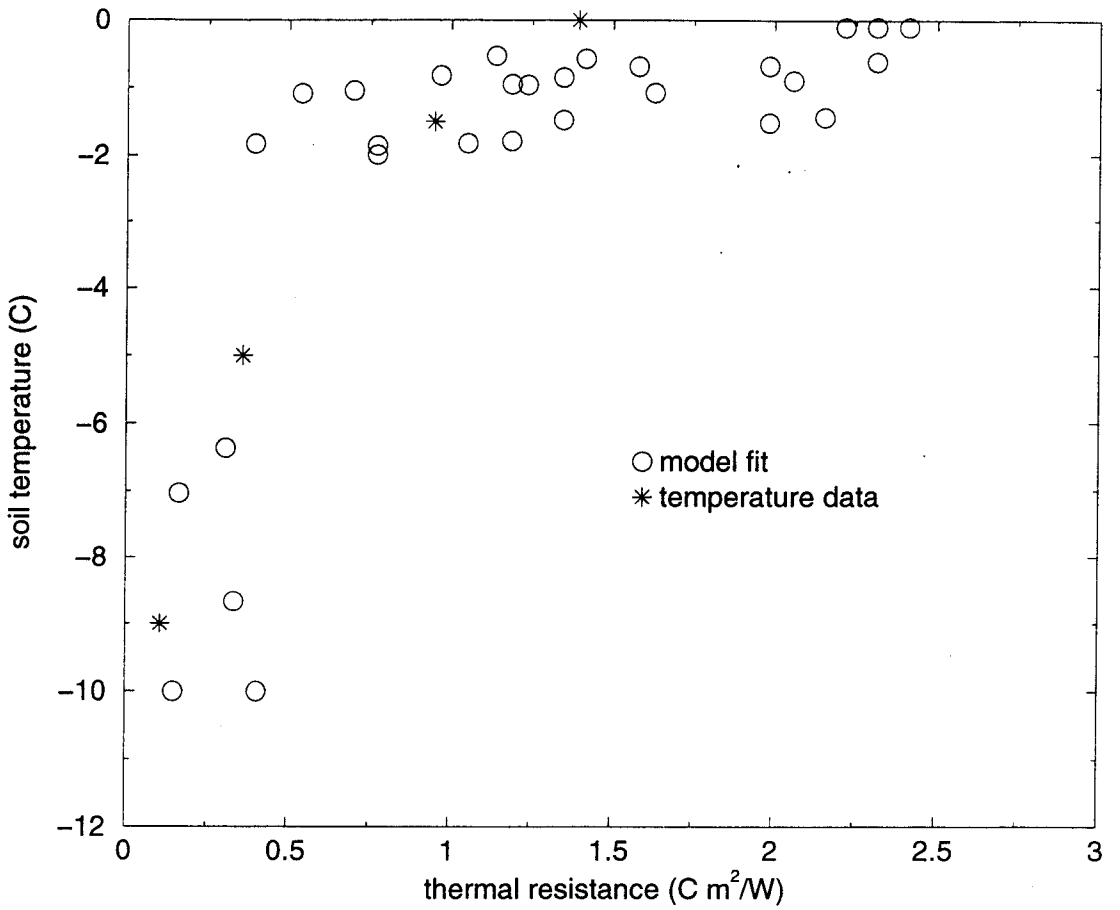

Figure 11: The soil temperatures used to generate the soil permittivites in Fig. 10 and the model results in Fig. 9. The soil is assumed to have a volumetric water content of 0.26 and the soil temperature is constrained to lie between -10 C and 0 C. Corresponding temperature measurements are plotted where available (see Fig. 8 in [Bernier and Fortin, 1998]).